

Numerical Simulation of Cavity Fuel Injection and Combustion for Mach 10-12 Scramjet

Dora E. Musielak
University of Texas at Arlington

ABSTRACT

We report the results from a study of cavity flame holding and its effect on combustion performance for a Mach 10-12 scramjet engine. We consider two distinct combustor configurations: (a) a constant cross section rectangular duct with a single cavity in the duct floor positioned at 15.3 cm downstream from the combustor's entrance, and (b) a diverging duct with a single cavity positioned at 7.1 cm from the entrance. For the later configuration, we evaluated two cavities: a shallow cavity with $L/D = 3$, and a deeper, larger cavity of $L/D = 4.94$. In both cases the rear ramp angle is 30° . To study the effect of fuel jet interaction with the cavity flow, the fuel injector was positioned at different locations inside and outside of the cavity. We found that when hydrogen is injected from the rear wall of the cavity, it mixes aided by a counterrotating vortex and the fuel reacts with the oncoming Mach 4.7 airstream, even at the fuel lean condition of this case ($f = 0.2$). However, the low fuel-to-air momentum flux ratio reduces the jet penetration into the main combustor airstream.

Keywords: cavity flame-holder, injection, scramjet flowpath, high-speed air-breathing propulsion

1 INTRODUCTION

In the past two decades, cavity flame holders have been proposed and studied by a number of researchers.^{1,2,3,4} Flame-holders are generally small recesses in the combustor wall with geometries characterized by their aspect ratio (L/D) and aft ramp angle (θ), as illustrated in Fig. 24. Key issues controlling the performance of cavity flame-holders include entrainment rate, residence time, and distribution of fuel and air within the cavity.⁵

Cavity flame-holders, designed by the Central Institute of Aviation Motors (CIAM) in Russia, were used for the first time in a joint Russian/French dual-mode hydrogen-fueled scramjet flight test.⁶ In 1994, NASA contracted with CIAM to continue exploring the axisymmetric scramjet operating envelope from dual-mode operation below Mach 6 to the full supersonic combustion mode at Mach 6.5 flight conditions. The combustor design includes two cavity flame-holders (20 mm in depth x 40 mm in axial length, and 30 x 53 mm).^{6,7,8,9,10} The performance predictions obtained by analytical and CFD solutions^{6,9} indicated that these cavities would be effective as autoignition and flame-holding devices. A flight test of the CIAM combustor in 1998 encouraged further investigation of cavities for scramjet application.

Although interest in cavity flame-holders has resulted in much research effort to determine their effectiveness for improving supersonic combustion, most of the results published to date have focused on experimental and computational studies with low speed, non-reacting flows. This provided a great opportunity to add to the knowledge base of these devices by carrying out an analytical study of cavity flame-holders at the higher Mach number conditions of the axisymmetric scramjet combustor under consideration. Thus, as

the study progressed, it was felt necessary to research the feasibility of adding a wall cavity for fueling the combustor. Two- and three-dimensional analysis of a combustor chamber with a wall cavity were carried out to assess whether injection through a cavity and in the vicinity of a cavity would provide additional flame stabilization and improve combustion. Some results of this analysis are reported in a separate paper.¹¹

2 COMPUTATIONAL TOOLS

The two- and three-dimensional flowfield and combustion characteristics resulting from hydrogen H₂ fuel injection through the cavities were simulated with the Viscous Upwind Algorithm for Complex Flow Analysis (VULCAN) code.¹² This NASA Navier-Stokes code was chosen for its demonstrated capability to model hypersonic turbulent reacting flows, incorporating multi-species, multi-reactions hydrogen-air finite rate kinetics models. The main mechanisms involved in fuel-air mixing are flow turbulence and molecular diffusion. VULCAN can model turbulent reacting flows over a wide range of conditions with a choice of several two-equation models such as Wilcox k-w model (1998 version) with or without the Pope correction term, and two-equation model of Menter based on Wilcox k-w model blended with Jones and Launder k-epsilon model.

The knowledge of the static temperature and of the species concentration in a reacting flow is indispensable for the understanding of the ignition and the reaction processes. VULCAN allows for an arbitrary chemical kinetic mechanism, specified as follows: The number of chemical reactions and the kinetic model data must be specified along with the number of chemical species. If finite rate chemistry is chosen, then the kinetic model data is specified through a kinetic model database file.

A 7 species/7 reaction hydrogen air kinetic model was used as baseline. Although more comprehensive reaction models can be used, for this preliminary study in which we were interested in tracking mainly the production of the flame species H₂O and OH to determine the extent of combustion, this simple 7-reaction model is adequate. No artificial ignition source was used.

Two different two-block structured grids were generated to span the computational domain representing the two models of the scramjet combustor. The first grid block spanning Combustor 1 has dimensions 193×129, for Combustor 2 the grid dimensions are 201×129; the second block spanning the cavity in both combustors has dimensions 65×57.

The following sections describe the two combustor configurations we selected for this study: 2-D and 3-D Scramjet with Cavity Fuel Injection.

3 2-D SCRAMJET WITH CAVITY INJECTION

3.1 Physical Model and Boundary Conditions

Table 1 summarizes the combustor flow conditions used in this work, which represent Mach 10-12 flight operation. We considered different fuel injection conditions to accommodate each freestream airflow condition. The fuel injection conditions are summarized in Table 2. For comparison and validation, the flow conditions for Cases 1 and 2 were taken from Neely.¹³

Table 1 - Air Flow Conditions

Case	Mach No.	Temperature (K)	Pressure (kPa)	Velocity (m/s)	Momentum Flux (kPa)
1 and 2	3.96	1563	97.8	3144	2166.9
3	4.66	1250	4.0	3216	122.6
4, 5, 6	3.38	1290	32.3	2438	520.3

Table 2 - Hydrogen Fuel Flow Conditions

Case	Temperature (K)	Pressure (kPa)	Velocity (m/s)	Momentum Flux (kPa)	Injector diam. (mm)	Injector Position	Cavity L/D
2	250	927.9	1203.0	1299.1	2.00	A	4.8
3	250	135.7	1203.6	189.98	1.39	B	3.0
4	246	487.0	1193.0	681.8	1.06	C	3.0
5	246	487.0	1193.0	681.8	1.66	D	3.0
6	246	487.0	1193.0	681.8	1.07	C	4.9

To study the effect of fuel jet interaction with the cavity flow, the fuel injector was positioned at different locations inside and outside of the cavity, as described in the Results section below.

For the first part of the analysis, two different combustor configurations were considered:

- (1) A 50 cm rectangular duct with a constant cross section (other than the cavity) of 2.2 cm. A single cavity was located in the duct floor at a distance of 15.3 cm from the leading edge of the combustor. The cavity (sketched below) has an aspect ratio $L/D = 6$ and a rear ramp angle of 22.5° (See Fig. 1). This combustor with cavity model was referred as “Combustor 1.”

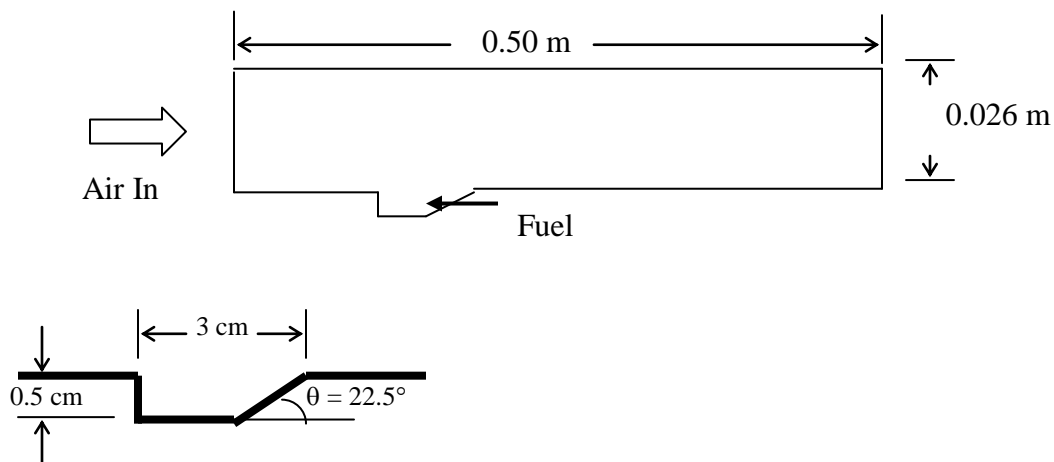


Figure 1. Computational Domain for Combustor 1 with Wall Cavity of $L/D = 6$.

- (2) A 24.6 cm long diverging duct with 2.6 cm average diameter. A single cavity was located in the combustor floor at a distance of 7.1 cm from the leading edge. Two cavities were analyzed: (1) a shallow small cavity with $L/D = 3$, and (2) a deeper, larger cavity of $L/D = 4.94$. In both cases the rear ramp angle is 30° (See Fig. 2). This combustor/cavity model was referred to as “Combustor 2.”

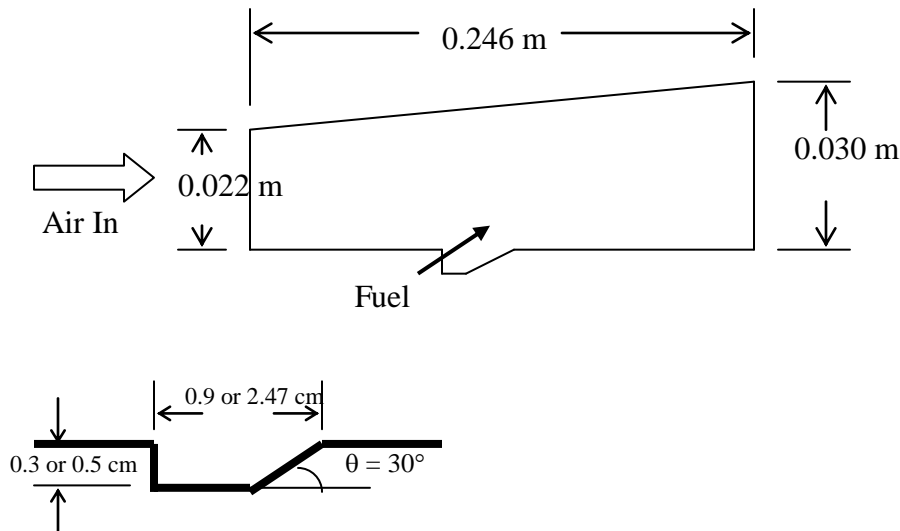


Figure 2. Computational Domain for Combustor 2 with Wall Cavity, $L/D = 3$ and 4.94 .

Many single-jet fuel injection cases were first analyzed, which served as calibration of the CFD code and provided the baseline data to scope the full simulations. The first 2-D analysis simulated the complexity of the interaction flowfield produced by a hydrogen jet injected into the cross flow of air at Mach 4.143 and 4.7, conditions representative of flight at Mach 10 and 12, respectively. Figure 3 shows the Mach number contours obtained for Case 1, compared with the schematic of the flow physics expected for transverse fuel injection flowfield.

The presence of the cavity and the injection of fuel both contribute to the formation of a structure of oblique shock waves in the scramjet combustor, which dominate the flowfield downstream of the cavity. Thus, in order to attain a better understanding of the flow physics inside the scramjet combustor, the initial test case models the effect of the cavity on the freestream air without the presence of the hydrogen fuel jet. This also helps to understand how the fuel jet affects that flow structure without combustion complicating the flowfield.

3.3 Results

The complexities of the high-speed reacting flow were simulated effectively, revealing significant interaction by the proximity of fuel jets that promoted mixing with the Mach 4.7 airstream.

3.3.1. Straight-Wall Combustor 1, Cavity with L/D = 6

Case 1: Fuel OFF

Upstream of the cavity, the boundary layer growth (from the sharp leading edge) generates only a weak wave structure. For this fuel-off case, the incoming flow enters the combustor at the given combustor inlet conditions. The shear layer created as the air flows over the cavity no longer remains parallel with the bottom wall, but is directed downwards and impinges on the inclined rear cavity face. A shock wave develops at this point, reflects off the top wall of the chamber, and so on. The process of reflecting off the walls occurs continuously along the long combustor, and this is observed with the strong fluctuations of wall pressure (see Figs. 3, 4). This pressure profile is similar and comparable to the pressure distribution reported by Neely, et al.³⁷ The flow characteristics inside and over the cavity for this case are illustrated with the Mach contours shown in Fig. 5.

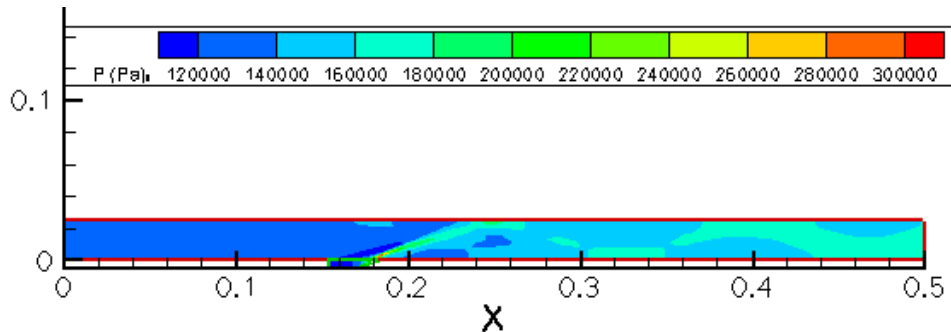


Figure 3. Pressure Distribution along Combustor 1, Case 1: Fuel Off.

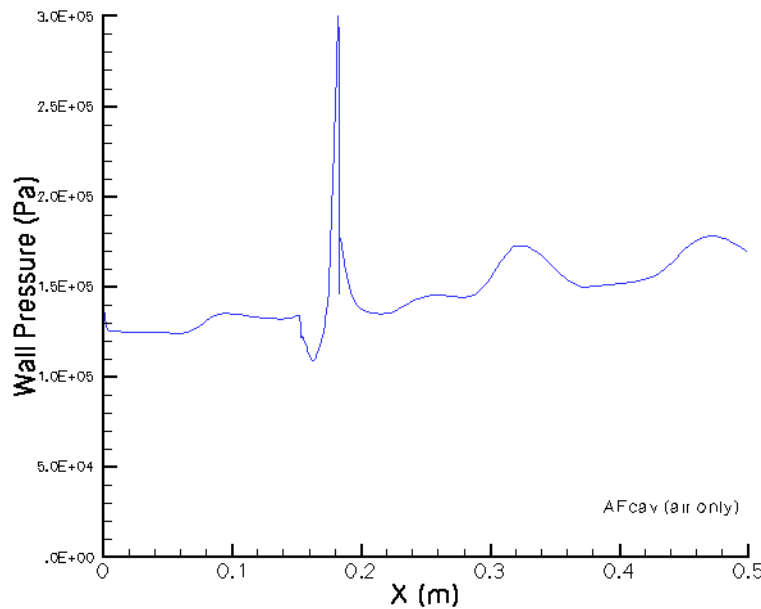


Figure 4. Wall Pressure Along Combustor 1 – Case 1: Fuel Off.

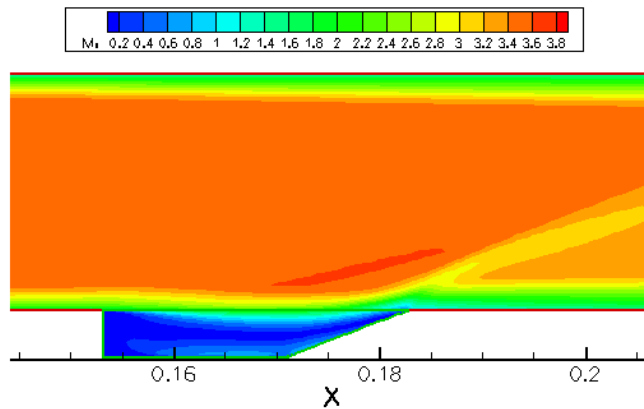
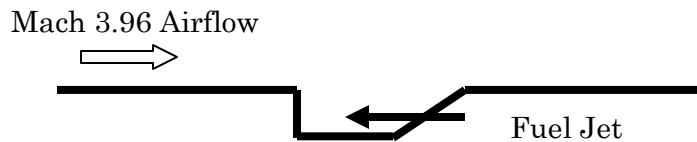


Figure 5. Flow Characteristics Inside and Over Cavity – Case 1: Fuel Off.

Case 2: Fuel ON

Hydrogen is injected from a 2 mm injector positioned at the rear (slanted) wall, inside of the cavity, as illustrated in the sketch below. Injection conditions are summarized in Table 2. Injector position A: at rear slanted cavity wall



In this case, the cavity is filled with fuel deflecting the shear layer out of the cavity. The fuel must leave the cavity (by conservation of mass); and thus, an obstruction is formed to the oncoming airflow. The incoming flow interacts with this jet/cavity obstruction, and it mixes with the fuel. A shock wave forms at the leading edge of the fuel bubble and reflects obliquely off the walls as it travels downstream, as illustrated by the Mach contours of Fig. 6. A subsonic region develops over the cavity and over the combustor wall immediately downstream, due to the strong shock created by both cavity and fuel jet interaction, which lifts the boundary layer of the incoming flow.

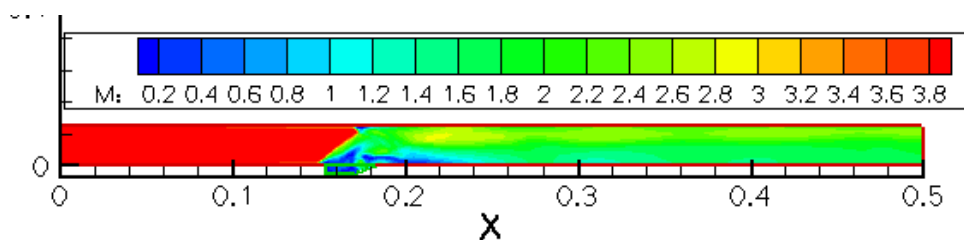


Figure 6. Mach Number Distribution in Combustor 1 – Case 2: Fuel On.

With this configuration, the cavity appears to be more effective for enhancing combustion. As shown in Fig. 7, the reaction zone (represented by H₂O mass fraction) is much wider and extends from the cavity all the way to the exit of the combustor. Combustion of the fuel in the shear layer above the cavity locally heats and expands the gas further, deflecting the oncoming flow with a stronger oblique shock.

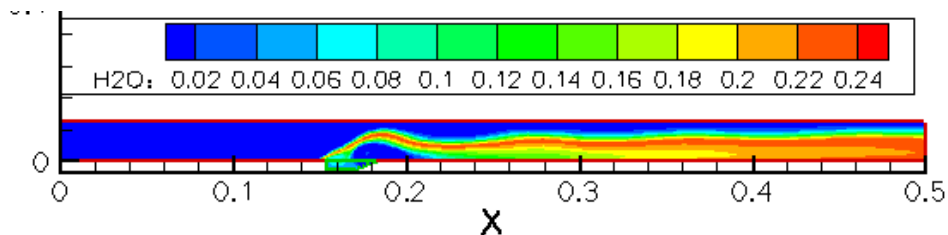
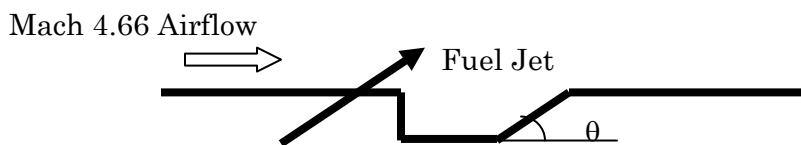


Figure 7. H₂O Mass Fraction Along Combustor (Case 2).

3.3.2. Diverging-Wall Combustor, Cavity with $L/D = 3$

Case 3: Fuel Injection from Combustor Wall, Upstream from Cavity – Injector at position B (bottom combustor wall, upstream from cavity).



For this case, a 1.39 mm fuel injector was placed 3 mm upstream of the cavity. As previously reported, a bow shock forms ahead of the fuel jet and interacts with the approaching boundary layer, resulting in a separation bubble. The separation region is 2-jet diameters ahead of the injector orifice. Interestingly, another separated region is present directly downstream of the fuel jet, i.e., the flow within the cavity is lifted by the effect of the jet.

As shown in Fig. 8, the reaction zone is much closer to the cavity, extending in a wider area as the flow reaches the exit of the combustion chamber. This would suggest a better performance of the cavity to hold the flame within the combustor at this condition. However, the mass fraction of H₂O is rather low (on the order of 16 percent), indicating that not all fuel has been thoroughly burned in the chamber.

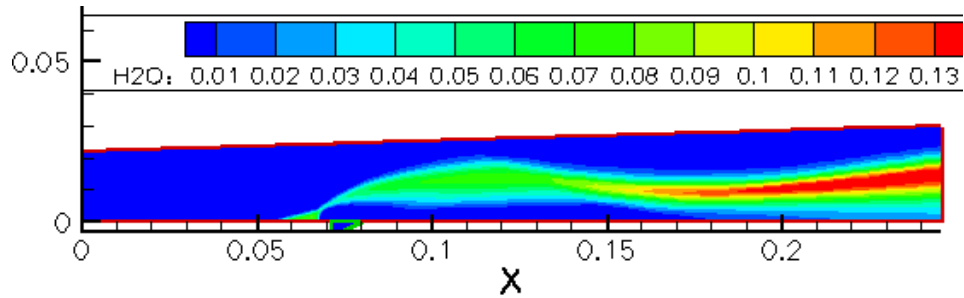
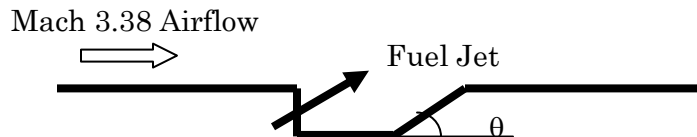


Figure 8. H₂O Mass Fraction Along Combustor (Case 3).

Case 4: Fuel Injection from Vertical Upstream Wall of Cavity - Injector position C: at front vertical wall



At the lower Mach combustor inlet condition, the performance of the $L/D = 3$ cavity is not very good. The flow structure in the chamber is typical. As shown in Fig. 9, the Mach number contours clearly indicate how the series of bow shocks develop at the left corner of the cavity, reflect on the top wall of the combustor, impinge on the lower wall, and so on. The amount of H₂O produced is at the lower limit of combustion (over 21 percent), but the reaction zone develops 10 cm downstream of the cavity and attains its highest value near the exit of the chamber, i.e., the cavity was not effective in holding the flame.

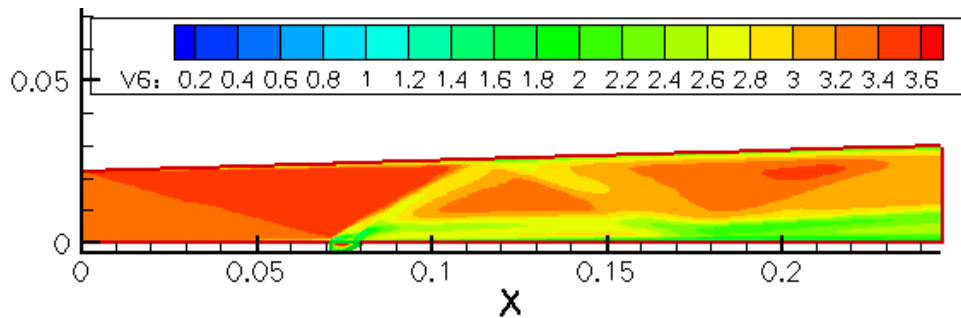


Figure 9. Mach Number Distribution in Combustor 2 – Case 4.

Case 5: Fuel Injection from Bottom Wall of Cavity Injector position D: at bottom of cavity.



As previously reported, when the fuel is injected from the bottom of the cavity, the flow structure inside and over the cavity are much different. Only one pre-combustion shock develops, which is caused by the airstream interacting with the first corner of the cavity. The bow shock impinges on the upper wall and is reflected. At the impingement point, a hot gas zone is observed, reaching the same order of magnitude temperature as the heat release zone of the pre-combustion shock. Also, the boundary layer separates a few millimeters from the cavity, and a separation bubble is also formed immediately after the downstream corner of the cavity.

The reaction zone is observed to develop downstream from the cavity, and it grows in intensity and size as it approaches the combustor exit (See Fig. 10).

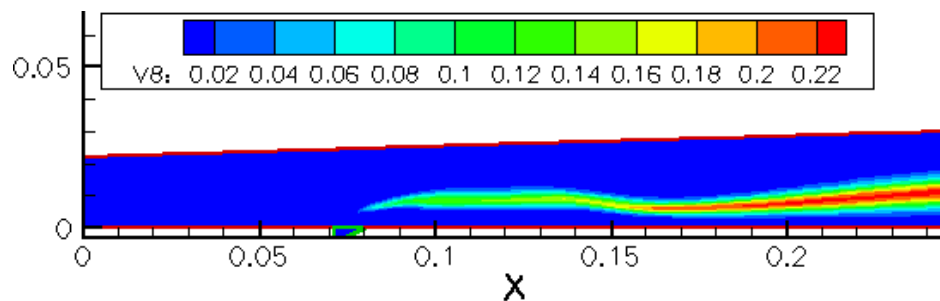
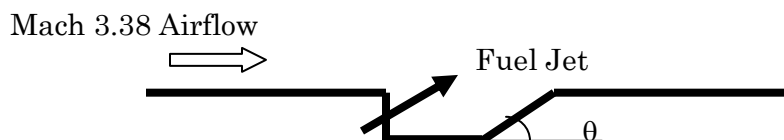


Figure 10. H₂O Mass Fraction Along Combustor (Case 5).

3.3.3. Diverging-Wall Combustor, Cavity with $L/D = 4.94$

Case 6: Fuel Injection from Vertical Upstream Wall of Cavity - Injector position C: at front vertical wall



The reaction zone, represented by the mass fraction of H₂O produced by the reaction of fuel with air, is observed further downstream from the cavity (See Fig. 11). The implication of this finding is that the cavity was not effective as a flame holder for this case.

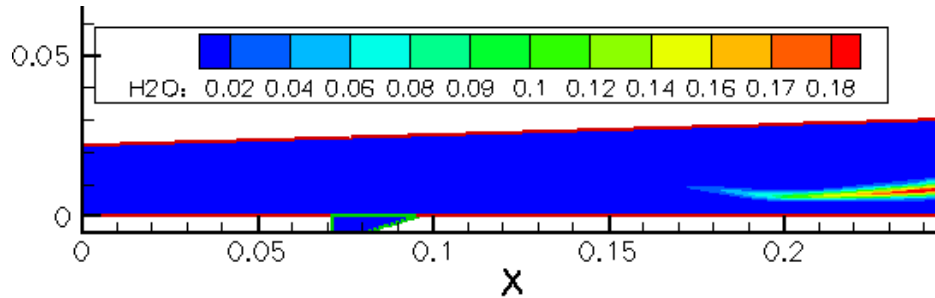


Figure 11. H₂O Mass Fraction Along Combustor (Case 6).

3.4 OBSERVATIONS

Long Straight-Wall Combustor 1, Cavity with L/D = 6

- Injecting the fuel from the right, slanted wall of the cavity appears to improve the flame-holding performance of the cavity. With this configuration, the increased amount of H₂O produced (above 26.7 percent), as well as the fact that the reaction zone begins immediately over the left corner of the cavity (Fig. 7) suggests that the presence of the cavity improves the conditions for air-fuel mixing and “holds” the flame effectively.

Short Diverging-Wall Combustor, Cavity with L/D = 3 and L/D = 4.94

- Comparing Cases 4 and 6, which have the same airflow conditions at the inlet of the combustor, the same fuel injection conditions, and the fuel injector is in the same position (left vertical cavity wall), it appears that raising the L/D from 3 to 4.94 of the cavity results in the worst flameholding characteristics. The magnitude of H₂O produced is slightly lower for the larger L/D cavity. (See Figs. 9 and 11).
- Comparing Cases 4 and 5, which have the same air and fuel conditions, with the only difference being the size and location of the fuel injector, it appears that the cavity performs better in Case 5 where the fuel is injected from the bottom wall of the cavity, as opposed to being injected from the left vertical cavity wall. Although the mass fraction of H₂O is about the same for the two cases, the fact that the reaction zone begins much closer to the cavity in Case 5 suggests that the size of the injector may not be as important as its location. This is also corroborated by the next conclusion. (See Figs. 9 and 10).
- Comparing Cases 3, 4, and 5, it is apparent that for the same L/D cavity, the size and location of the reaction zone is dependant on the location of the injector. The reaction zone is wider and closer to the cavity for Case 3, for which the injector was located upstream from the cavity proper. This also seems to suggest that the reaction develops as a result of the fuel jet interacting with the bow shock that forms over the cavity. (See Figs. 8, 9, and 10)

4. 3-D COMBUSTOR WITH CAVITY

4.1 Introduction

No adequate mechanism exists to help determine the effectiveness of cavities for scramjet flame-holding applications. Perfectly-stirred reactor (PSR) calculations may not be adequate as the cavity flowfield is complex and the fuel-air mixture may not be well mixed.³⁷ Thus, the effectiveness of the cavity in the three-dimensional, Mach 4.7 combustor is derived from a qualitative assessment of the combustion characteristics, as explained below.

4.2 Physical Model and Boundary Conditions

For the 3-D analysis, the computational domain consists of a 50 cm rectangular duct with a constant cross section (other than the cavity) of 2.2 cm. A cavity is located in the duct floor at a distance of 15.3 cm from the leading edge of the combustor. The cavity has an aspect ratio $L/D = 6$ and a rear ramp angle of 22.5° (See Figure 1). The fuel is injected from the slanted cavity wall in the direction opposite to the freestream air. This combustor/cavity geometry considered in this study was taken from Neely, et.al.¹² The conditions in the combustor are listed in Table 3.

A structured four-block grid was used, sized with over 1.4 million grid cells. The mesh was refined near the surfaces that represent solid walls. All top and bottom surfaces are assumed to be no slip isothermal walls. The size of the fuel orifice was chosen to give mass flow rates yielding an overall equivalence ratio of 0.2. Supersonic outflow boundary with zeroth order extrapolation of all variables was specified at the exit of the chamber.

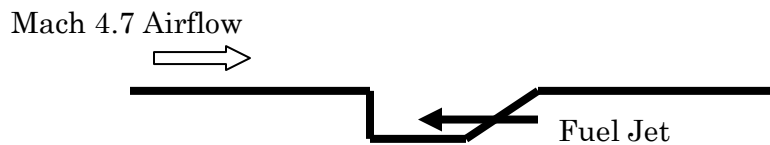


Table 3 - Combustor Conditions

<i>Analysis</i>	M_3	T_3 (K)	P_3 (kPa)	T_f (K)	P_f (kPa)	ϕ
3-D	4.7	1300	50.849	350	310.36	0.2

4.3 Results

When hydrogen is injected from the rear wall of the cavity, it mixes and reacts with the oncoming Mach 4.7 airstream, even at the fuel lean condition of this case ($f = 0.2$). The low penetration of the fuel jet into the main combustor airstream is the result of the low fuel-to-air momentum flux ratio. However, a small counter-rotating vortex is formed on each side of the fuel jet, represented by the +/- contours of tangential velocity component, that promotes mixing. This is a feature of the flowfield that was not possible to capture with the simple 2-D analysis.

The three dimensionality of the cavity flow is evident by the lateral spreading of the mixture. Figure 12 shows the 3-D combustor flowfield, represented with a highly compressed view in the x -direction. The figures show y - z slices at several axial stations along the combustor. As shown, the reaction zone begins where the fuel jet leaves the cavity and spreads laterally in a thin layer over the cavity trailing edge. The bulk of water vapor is found downstream, extending throughout the length of the combustor, very much as it was observed with the 2-D analysis.

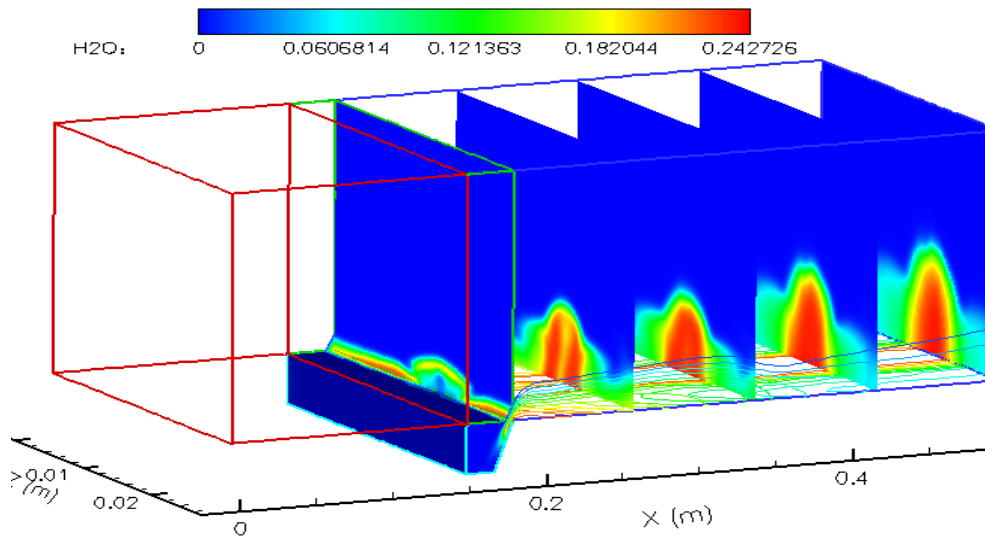


Figure 12. H_2O Mass Fraction Distribution in $M_3 = 4.7$ Combustor.

The ignition zone, represented by the mass fraction of OH produced, does not originate upstream of the cavity, as it was predicted for the lower Mach case using 2-D analysis. As shown in Fig. 13, OH is first detected along the trailing edge of the cavity, spreading out in the z -direction, on each side of the fuel jet. Some OH is formed on the sides of the reactive mixture that flows downstream; no OH is observed inside the cavity. These results are consistent with those of Neely et al.¹² who noted that no radicals were entrained into the cavity by recirculation, a conclusion they reached from both CFD prediction and examination of PLIF images.

Shown in Figure 14 is the wall pressure, normalized with the burner entrance pressure, calculated at the z -plane that crosses through the middle of the hydrogen jet. The profile is consistent with the observations of a shock train that develops in the chamber, i.e., a low pressure region at the bottom of the cavity, followed by a compression wave at the trailing edge, and then reflection over the top combustor wall, and so on.

Although steady state CFD models cannot capture the unsteadiness that is inherent in supersonic combustors with cavity fuel injection, these simulations provide invaluable insight into the complex reacting flow fields in the combustor. Once validated with relevant data, these results will guide the design of an effective fuel injection system for the Mach 10-12 scramjet-powered vehicle under consideration.

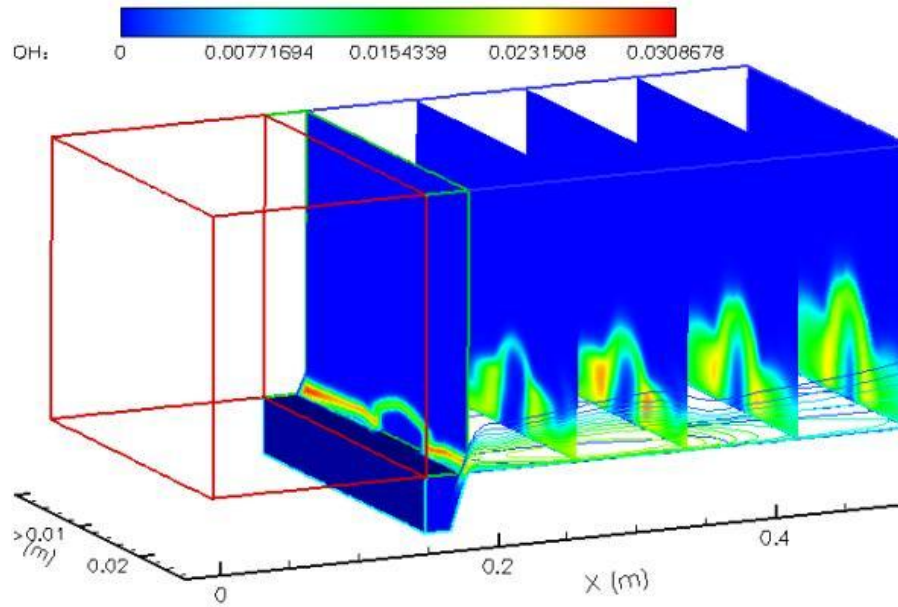


Figure 13. OH Mass Fraction Distribution in $M_3 = 4.7$ Combustor.

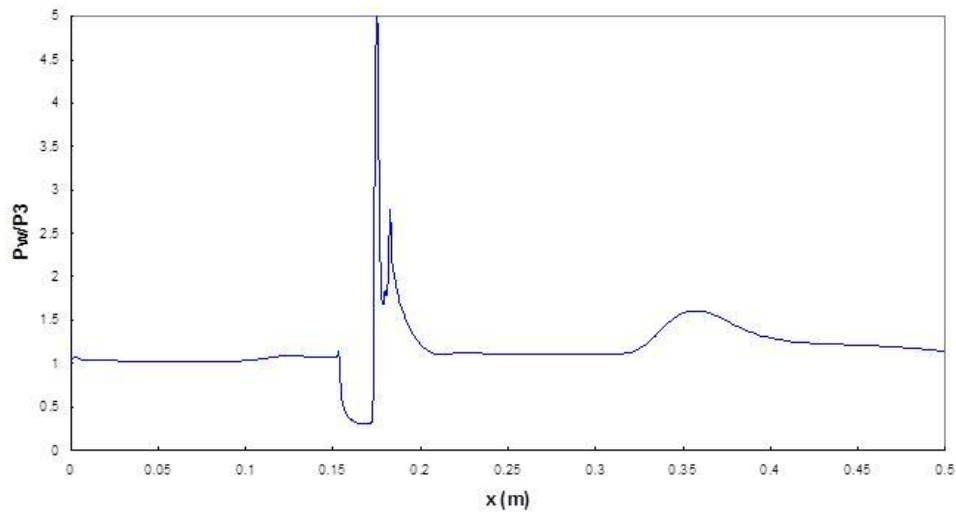


Figure 14. Normalized Wall Pressure along Combustor with Cavity.

5. CONCLUSIONS

- **2-D Combustor with Cavity Fuel Injection:**

The size of the cavity, diameter of the fuel injector, and injector position with respect to the cavity are all closely coupled. No mechanism exists to help determine the effectiveness of cavities for scramjet flame-holding applications. However, based on the 2-D results

obtained thus far, the location of the fuel injector with respect to the cavity has a marked effect on the flame-holding characteristics of the cavities studied. Furthermore, the cavity/fuel injection configuration represented in one particular case has greater potential to improve the mixing and combustion characteristics of the long constant-cross section combustor. Also, this configuration was intended to be tested with the short, diverging combustor to see if combustion is enhanced by injecting the fuel from the rear, slanted wall on the right side of the cavity.

Predictions for a Mach 3.96, 2-D combustor with cavity hydrogen injection at stoichiometric conditions suggested that some degree of combustion takes place inside the cavity. But the reaction layer is strongest at the leading edge and in the mixing layer that develops over the cavity. The reaction then spreads axially throughout the entire length of the chamber.

- **3-D Combustor with Cavity Injection**

The three-dimensional combustor flowfield that develops from the interaction of H₂ fuel injected through a wall cavity into Mach 4.7 air was characterized. The complexities of the reacting flow were simulated effectively, revealing more physical details of the fuel jet mixing with the high velocity airflow. It was found that the hydrogen jet autoignites above the cavity, and the reaction zone spreads downstream throughout the combustion chamber.

The 3-D steady state CFD simulations of a Mach 4.7 combustor with substoichiometric hydrogen injection do not predict OH or H₂O inside the cavity. This analysis predicts that a mixing layer develops right over the trailing edge of the cavity, where the reaction begins around the jet plume emerging from the cavity, and it spreads laterally in the z-direction, and also axially downstream from the cavity. These results are consistent with those reported in the literature, resulting from both CFD prediction and experiments conducted at comparable conditions and with the same combustor/cavity geometry.

Although steady state CFD models cannot capture the unsteadiness that is inherent in supersonic combustors with cavity fuel injection, these simulations provide invaluable insight into the complex reacting flow fields in the combustor. Once validated with relevant data, these results will guide the design of an effective fuel injection system for the Mach 10-12 scramjet-powered vehicle under consideration.

ACKNOWLEDGMENT

I wish to thank NASA, and in particular R. Baurle from NASA Langley Research Center for providing the VULCAN code to perform this analysis.

REFERENCES

¹ Tishkoff, J.M., Drummond, J.P., Edwards, T., and Nejad, A.S., "Future Direction of Supersonic Combustion Research: Air Force/NASA Workshop on Supersonic Combustion," AIAA Paper 97-1017, Jan. 1997.

² Mathur, T., Streby, G., Gruber, M., Jackson, K., Donbar, J., Donaldson, W., Jackson, T., Smith, C., and Billig, F. "Supersonic Combustion Experiments with a Cavity-Based Fuel Injector." AIAA Paper 99-2102, June 1999.

-
- ³ Gruber, M., Jackson, K., Mathur, T., Jackson, T., and Billig, F. "A Cavity-Based Fuel Injector / Flameholder for Scramjet Applications." 35th JANNAF Airbreathing Propulsion Subcommittee and Combustion Subcommittee Meeting, 1998, 383-397.
- ⁴ Gruber, M. R., Baurle, R. A., Mathur, T., and Hsu, K.-Y. "Fundamental Studies of Cavity-Based Flameholder Concepts for Supersonic Combustors." AIAA Paper 99-2248, June 1999.
- ⁵ K.-Y. Hsu, C. Carter, J. Crafton, M. Gruber, J. Donbar, T. Mathur, D. Schommer, and W. Terry, "Fuel Distribution About a Cavity Flameholder in Supersonic Flow," AIAA-2000-3585.
- ⁶ Roudakov, A.S., Schikhmann, Y., Semenov, V., Novelli, P., and Fourt, O., "Flight Testing of an Axisymmetric Scramjet – Russian Recent Advances," IAF Paper 93-S.4.485, Oct. 1993.
- ⁷ McClinton, C., Roudakov, A., Semenov, V. and Kopchenov, V., "Comparative Flow Path Analysis and Design Assessment of an Axisymmetric Hydrogen Fueled Scramjet Flight Test Engine at Mach 6.5," AIAA Paper AIAA-1996-4571.
- ⁸ Roudakov, A., Semenov, V. and John W. Hicks, "Recent flight test results of the joint CIAM-NASA Mach 6.5 scramjet flight program," AIAA Paper AIAA-1998-1643.
- ⁹ Rodriguez, C. "CFD Analysis of the NASA/CIAM Scramjet," AIAA-2002-4128.
- ¹⁰ Volland, R.T., A. H. Auslender, M. K. Smart, A. S. Roudakov, V. L. Semenov, and V. Kopchenov, "CIAM/NASA Mach 6.5 scramjet flight and ground test," AIAA Paper AIAA-1999-4848.
- ¹¹ Musielak, D.E. and Micheletti, D., "Numerical Simulation of Cavity Flame Holders for Combustion and Flame Stabilization in a Mach 10-12 Scramjet Vehicle." Presented at the 2006 JANNAF CS/APS/PSHS Joint Meeting, San Diego, CA, December 4-8, 2006.
- ¹² White, J.A. and Morrison, J.H., "A Pseudo-Temporal Multi-Grid Relaxation Scheme for Solving the Parabolized Navier-Stokes Equations," AIAA Paper No. 99-3360, June 1999.
<http://vulcan-cfd.larc.nasa.gov/WebPage/aiaa99-3360.pdf>
- ¹³ Neely, A.J., Riley, C., Boyce, R.R., Mudford, N.R., Houwing, A.F.P., and Gruber, M. R., "Hydrocarbon and Hydrogen-Fuelled Scramjet Cavity Flameholder Performance at High Flight Numbers." AIAA Paper 2003-6989, December 2003.